

# Wind Power Collection and Transmission with Series Connected Current Source Converters

Hak-Jun Lee, and Seung-Ki Sul

School of Electrical Engineering & Computer Science, Seoul National University

130 dong, Daehak-dong, Gwanak-gu, 151-744

Seoul, Korea

Tel.: +82 / (2) – 880-7991.

Fax: +82 / (2) – 883-0827.

E-Mail: [hjlee@eepel.snu.ac.kr](mailto:hjlee@eepel.snu.ac.kr), [sulsk@plaza.snu.ac.kr](mailto:sulsk@plaza.snu.ac.kr)

URL: <http://eepel.snu.ac.kr>

## Keywords

«Wind power», «Current source converter», «CSC», «HVDC».

## Abstract

In this paper, series connected DC current source converter based Wind Turbine Generation System (WTGS) is proposed. Not only a multi-phase generator but also a group of wind turbine generator can be linked easily with multiple series connected current source converters. It is expected that the system can have higher availability and lower initial setup cost compared to conventional voltage source converter based WTGS. The modeling and the control strategy for the proposed system is investigated. A 3 MW system with three series connected current source converters has been simulated by the computer program. The effectiveness of the proposed control strategy is verified by the simulation.

## Introduction

The demand of sustainable and renewable energy has been increased remarkably due to the energy crisis and the environmental concern. Among the various renewable energy sources, especially, the wind energy capacity has been increased rapidly over the last ten years. According to the recent research, the installed wind power capacity is expected to reach close to 200 GW by the end of 2010 with around 40 GW of new capacity added in 2010 alone. The research also forecasts that global wind power capacity will be reached more than 400 GW between 2010 and 2014 [1].

Because of the cost issue, mechanical stress, control performance and etc, the technology for wind turbine generator system has evolved from fixed speed generator to adjustable speed generator (ASG). Among the ASGs, the doubly fed induction generator (DFIG) has been used most widely because of the reduced size and cost of power converter and harmonic filter, and improved efficiency [2]. However, with the deep penetration of Wind Turbine Generation System (WTGS), the stringent Grid Code is applied to newly constructed WTGS. And under the Grid Code, the cost effectiveness of DFIG cannot be maintained any more [3]. To enhance the efficiency and reliability of overall system as well as to meet Grid Code, multi-pole/phase Permanent Magnet Synchronous Generator (PMSG) with full scale power converter has appeared as a main stream in gearless WTGS [4]-[5].

With the increased demand of the wind power, large scale wind farm, over hundreds MW, has been constructed with many WTGSs. In addition, the capacity of a unit WTGS has been increased rapidly. Nowadays, the largest capacity for the commercial WTGS has been up to 5 MW [6]. As the capacity of WTGS increases, to reduce current level, the medium voltage system has been adopted for power converters and generators of WTGS. To enhance the quality of wind itself and reduce environmental issue, the wind farm has been constructed in a site far distant from urban or in an offshore. Thus, there are many studies for collection and transmission of the generated electricity from the large scale wind farm to the existing utility grid [3].

This paper introduces a series connected DC current source system for variable speed full scale WTGS as an alternative to the conventional voltage source based parallel connected system. To implement the

DC current source, the current source converter (CSC) is adopted. Traditionally, the CSC had been used for the high power drives due to its ruggedness to over current / short circuit and low  $dv/dt$  voltage stress over the stator windings [7]-[8]. In addition, the series connection can be easily implemented by CSCs because of inherent characteristics of controlled current on the contrary to the voltage source converter (VSC), where the current is set by the external circuit. And, with the series connection of multiple CSCs connected to multi-phase PMSG, the medium voltage system can be easily implemented even using low voltage switching devices. On the other hands, due to the filter capacitor in CSC, the CSC-fed drive system has inherent issue with LC resonance. In order to attenuate the LC resonance, the multi-loop current controller is proposed in this paper. To evaluate the performance of the proposed system, computer simulation has been performed using PSIM® software.

## System description

### CSC configuration with IGBT-diodes

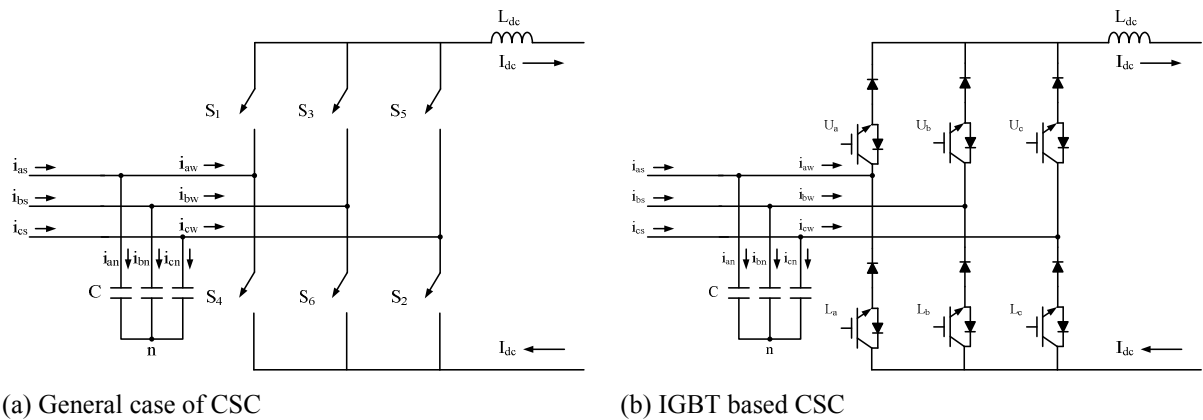


Fig. 1: Circuit diagram of Current Source Converter (CSC) with the input capacitor filter and DC link inductor

Fig. 1 (a) depicts a circuit diagram of the CSC. The CSC consists of six controllable power semiconductor switches which have unidirectional current conduction and bidirectional voltage blocking capabilities, and DC-link inductor as an energy storage element. The three phase filter capacitor,  $C$ , is required for the commutation of switching devices and filtering out the current harmonics. As the controllable power semiconductor switch, gate turn-off thyristor (GTO) or integrated gate commutated thyristor (IGCT) or insulated gate bipolar transistor (IGBT) with diode can be employed. There was a comparative study with consideration on selection of power semiconductors [9]. Because the cost and size of the passive components would be reduced as the switching frequency increases, in this paper, the IGBT based CSC is adopted to increase the switching frequency more than 1 kHz even in MW drive system [9]. The IGBT based CSC can be described as shown in Fig.1 (b).

### Proposed structure for single wind turbine generator with multi-phase PMSG

As shown in Fig. 2, the constant DC-link current,  $I_{dc}$ , flows to receiving network while the voltage across DC-link is the sum of the back EMF voltages of PMSG. The voltage across DC-link is varied with power from PMSG which is determined by the wind speed. Because each CSC has same level of DC-link voltage in single wind turbine generator, the total DC-link voltage,  $V_{total}$ , is proportional to the number of 3-phase winding. If it is assumed that the  $(3 \times n)$ -phase PMSG is used for single wind turbine generator than the total DC-link voltage can be expressed by (1) and (2).

$$V = \frac{P_{wind}}{I_{dc}} \quad (1)$$

$$V_{total} = n \times V \quad (2)$$

where  $P_{wind}$  : generated power from each 3-phase windings.

Thus, the medium voltage system can be easily implemented using low voltage switching devices with Series Connected CSC (SCCSC) for multi-phase PMSG.

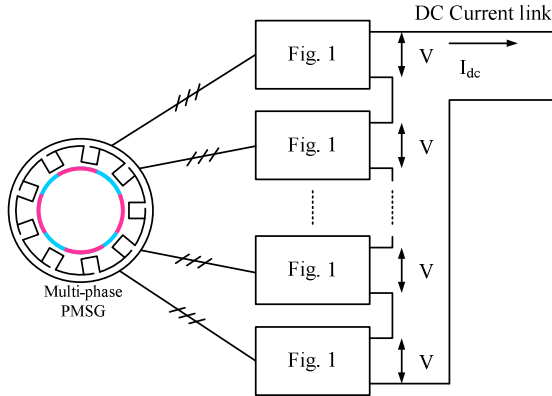


Fig. 2: Series connected CSC for multi-phase PMSG

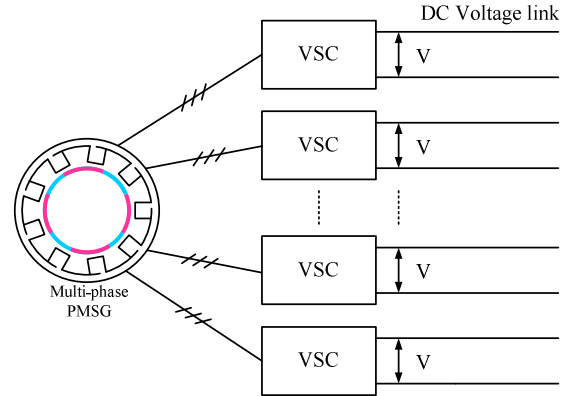


Fig. 3: Conventional Parallel connected VSC for multi-phase PMSG

The SCCSC has a duality with parallel connected VSC which was already introduced in [10].

Fig. 3 shows the parallel connected VSC for multi-phase PMSG. It has the same concept with SCCSC. However, the number of DC-link line with low voltage level increases as the number of phases of PMSG increases. Thus, it might be not cost effective solution for several MW WTGS in the aspect of the cost and size.

### Topology to transmit the generated power from multiple WTGSs to grid

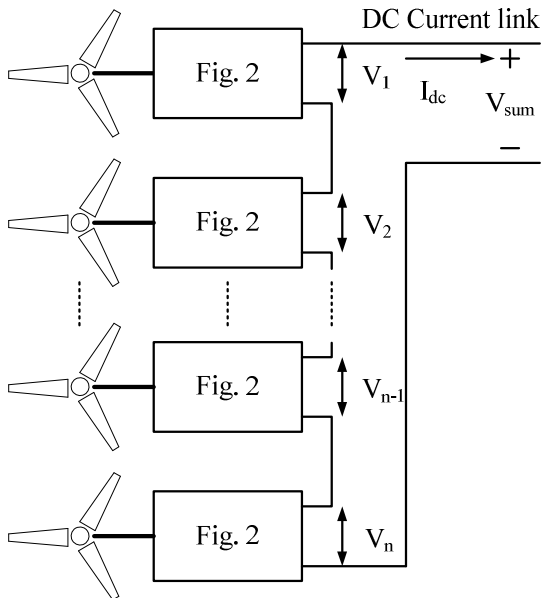


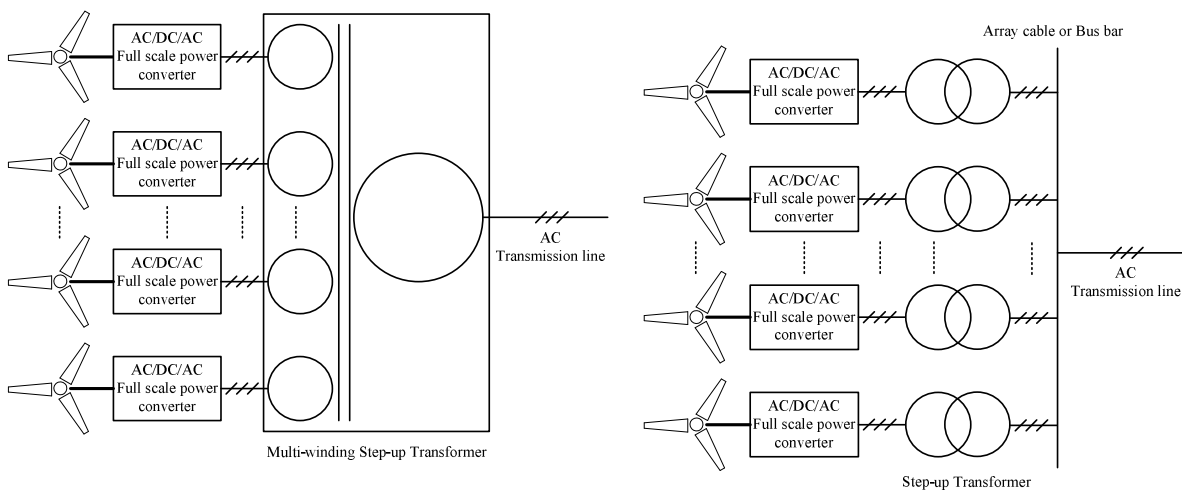
Fig. 4: Series connected CSC for integrating multiple WTGS

As shown in Fig. 4, each wind turbine generator in a wind farm can be integrated with SCCSCs. The voltage across DC-link of single WTGS can be connected in series as the same manner of the case of multiple phases SCCSC system for single wind turbine generator. Because the overall wind turbine generator share the same DC-link current, it is possible that each single SCCSC system has different DC-link voltage with different generated power. The power generated by a wind turbine can be expressed as (3).

$$P = \frac{1}{2} \rho \pi R^2 V_{wind}^3 C_p \quad (3)$$

where  $\rho$ : air density,  $R$ : turbine rotor radius,  $V_{wind}$ : wind speed, and  $C_p$ : turbine power coefficient. From (3), it can be seen that the power generated by a wind turbine is proportional to the cubic of the wind speed. It means that each WTGS operating with different wind speed generates different power and the sum of voltage of each WTGS,  $V_{sum}$ , would vary under the same DC link current. The total generated power can be transmitted via the medium DC voltage,  $V_{sum}$ , whose magnitude would vary according to the wind speed. The variation can be reduced by adjusting the DC link current appropriately. For this integration of WTGSs, each three phase winding of PMSG should be insulated to the level of the transmission voltage,  $V_{sum}$ . And, the transmission voltage would be limited by the possible insulation level of the each windings of PMSG. Under the consideration of the practical medium voltage insulation technique of the electric machine, the voltage can be increased up to several tens of kV with reasonable cost.

On the contrary, in the case of VSC concept, the parallel connection is available choice to integrate the wind turbine generators in wind farm. The transformer has been usually used for integrating the wind turbine generators as shown in Fig. 5.

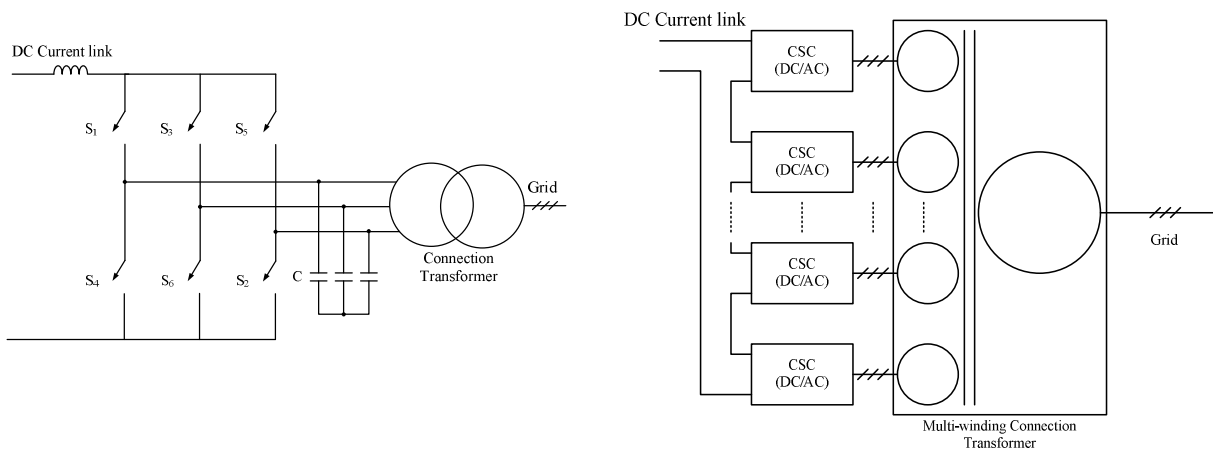


(a) With multi-winding step-up transformer

(b) With step-up transformer and array cable

Fig. 5: Parallel connected VSC for integrating WTGS

Due to the multi-winding step-up transformer as shown in Fig. 5 (a), or the step-up transformer and array cable such as bus bar connection as shown in Fig. 5 (b), the size and initial setup costs of WTGS in wind farm of VSC based system would be drastically increased. Additionally, in the case of VSC system for multi-phase PMSG, it is required the additional transformer or inductor for parallel connection of separate VSC in AC/DC/AC full scale power converter.



(a) With single CSC

(b) With multiple SCCSCs and multi-winding step-up transformer

Fig. 6: Interconnection method with electric grid

## SCCSC for grid connection

There are several choices in order to interconnect the DC transmission line of SCCSC with the utility grid. One is the high-capacity CSC and other is the SCCSC with multi-winding connection transformer. Fig. 6 (a) depicts the interconnection of the DC transmission line with the utility grid by a single high-capacity CSC. The controllable switch can be implemented with series connected switching devices such as IGCT, GTO and IGBT with diode module. Because of the reliability and difficulty of control for series connected switching devices, as the system shown in Fig. 6 (b), where the SCCSCs is connected to the grid through a multi-winding transformer, might be a viable solution for the interconnection.

As like full-scale VSC, the control of power factor at grid side is possible regardless of wind turbine generator side because the generators are decoupled from grid by DC current link. Thus, SCCSC system has capability to meet the Grid Code.

## Protection of the SCCSC system against external faults

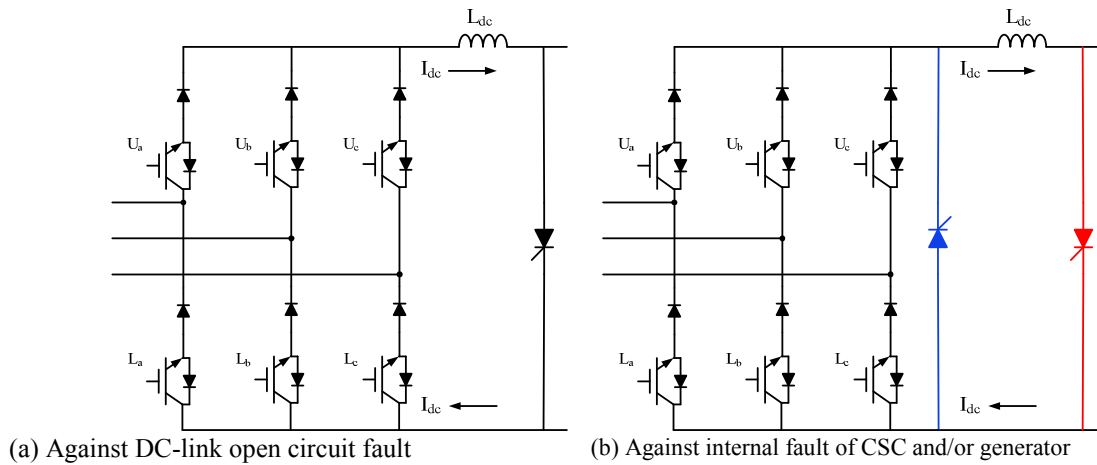


Fig. 7: Protection method of SCCSC

The protection is important issue for WTGS. Basically, the CSC has ruggedness to short circuit due to the DC link inductor. The proposed SCCSC system has medium voltage DC-link tied directly to a transmission line. Because of the inherent advantage of CSC, the DC link short circuit cannot be considered as severe system fault. While the DC link open circuit would be rather severe system fault to SCCSC. As shown in Fig. 7 (a), to prevent DC link open circuit, the power semiconductor switch can be installed to each CSC in parallel as a crow-bar. If the transmission line is suddenly open circuited, the thyristor would be turned on and the current in the DC-link inductor can be circulated. In addition, if each wind turbine generator and/or the corresponding CSC have any internal fault, another thyristor shown in Fig. 7 (b) would be turned on to bypass the faulty CSC and generator. In these ways, the faulty CSC can be detached from SCCSC system, and the continuous operation with all other healthy CSCs and generators is guaranteed.

## Modeling of CSC Including PMSG and Capacitor Filter

The CSC-fed PMSG can be modeled as (4)-(6) in the rotor reference d-q frame.

$$\begin{bmatrix} i_{dw}^r \\ i_{qw}^r \end{bmatrix} = \begin{bmatrix} i_{ds}^r \\ i_{qs}^r \end{bmatrix} + \begin{bmatrix} i_{dn}^r \\ i_{qn}^r \end{bmatrix} \quad (4)$$

$$\begin{bmatrix} i_{dn}^r \\ i_{qn}^r \end{bmatrix} = \begin{bmatrix} pC_s & -\omega_r C_s \\ \omega_r C_s & pC_s \end{bmatrix} \begin{bmatrix} v_{ds}^r \\ v_{qs}^r \end{bmatrix} \quad (5)$$

$$\begin{bmatrix} v_{ds}^r \\ v_{qs}^r \end{bmatrix} = \begin{bmatrix} R_s + pL_{ds} & -\omega_r L_{qs} \\ \omega_r L_{ds} & R_s + pL_{qs} \end{bmatrix} \begin{bmatrix} i_{ds}^r \\ i_{qs}^r \end{bmatrix} + \begin{bmatrix} 0 \\ \omega_r \lambda_{PM} \end{bmatrix} \quad (6)$$

where  $i_{dqw}^r$  : d and q axis output current of CSC,  $i_{dqs}^r$  : d and q axis stator current of PMSG,  $i_{dqm}^r$  : d and q axis current of filter capacitor,  $v_{dqs}^r$  : d and q axis voltage of filter capacitor,  $R_s$  : stator resistance of PMSG,  $L_{ds}$ ,  $L_{qs}$  : d and q axis synchronous inductance of PMSG, respectively,  $\omega_r$  : rotor angular speed of PMSG,  $\lambda_{PM}$  : flux linkage by permanent magnet and  $p$  : derivative operator. In the case of the modeling of CSC-fed grid,  $\omega_r$  stands for the angular speed of grid voltage and  $\omega_r \lambda_{PM}$  stands for the peak phase voltage of grid voltage.

From those equations, the equivalent circuit of CSC including PMSG and capacitor filter can be derived as shown in Fig. 8.

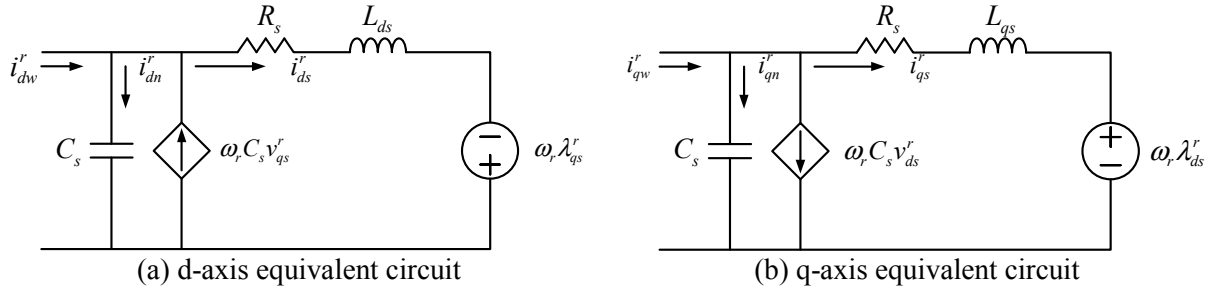


Fig. 8: Equivalent circuit of CSC including PMSG and capacitor filter

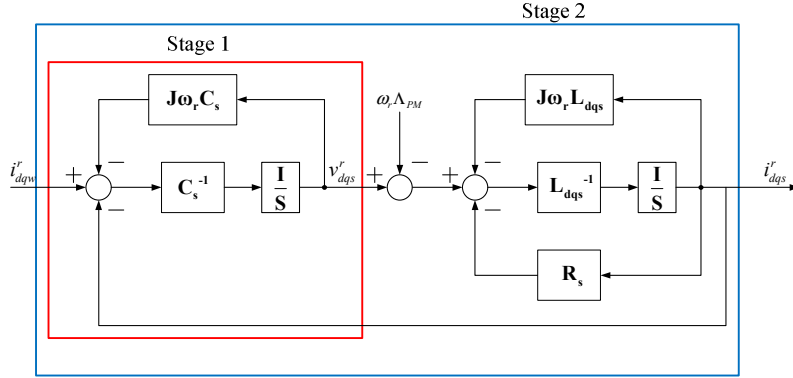


Fig. 9: Control block diagram of CSC including PMSG and capacitor filter

The equivalent circuit in Fig. 8 can be simply expressed as a control block diagram as shown in Fig. 9.

### Current regulator design

The multi-loop controller can be applied to control the output of a higher order plant such as the CSC-fed PMSG system with LC filter. To reduce the passive components, such as DC-link inductor, filter inductor, and filter capacitor, as well as to suppress the resonance due to LC filter of CSC, the precise current control might be important issue. In this paper, the multi-loop current controller based on two stages modeling of the CSC-fed PMSG, shown in Fig. 11, is proposed. As the current regulator, simple PI controller is used and its gains are set as the technical optimum, which cancel the pole of plant by the zero of the controller. With this controller, the transfer function between the actual stator current and its reference can be designed as the 2<sup>nd</sup> order low pass filter. The gains of the current controller can be easily determined by LC parameters of CSC.

The current controller can be designed using the block diagram in Fig. 10. To control  $v_{dqs}^r$  in the first stage, simple P controller can be introduced where the coupling term is decoupled by the feed-forwarding term. In the second stage, the PI controller can be used to control stator current of PMSG,  $i_{dqs}^r$ , where the coupling term can be decoupled by the integrator with coupling error term which was already introduced as a complex vector current control concept [11].

The transfer function of the first stage can be set as the 1<sup>st</sup> order low pass filter with P controller. The output of the controller can be expressed by (7) where superscript ‘\*’ stands for the reference and  $K_{pv}$  stands for the proportional gain.

$$\begin{bmatrix} i_{dw}^r \\ i_{qw}^r \end{bmatrix} = \begin{bmatrix} K_{pv} & 0 \\ 0 & K_{pv} \end{bmatrix} \begin{bmatrix} v_{ds}^r - v_{ds}^r \\ v_{qs}^r - v_{qs}^r \end{bmatrix} + \begin{bmatrix} i_{ds}^r \\ i_{qs}^r \end{bmatrix} + \begin{bmatrix} 0 & -\omega_r C_s \\ \omega_r C_s & 0 \end{bmatrix} \begin{bmatrix} v_{ds}^r \\ v_{qs}^r \end{bmatrix} = \begin{bmatrix} i_{ds}^r \\ i_{qs}^r \end{bmatrix} + \begin{bmatrix} sC_s & -\omega_r C_s \\ \omega_r C_s & sC_s \end{bmatrix} \begin{bmatrix} v_{ds}^r \\ v_{qs}^r \end{bmatrix} \quad (7)$$

If the feed-forwarding term is well matched to the coupling term of the real plant and the current reference is the same with the synthesizing current of CSC, then the transfer function in the first stage can be set as 1<sup>st</sup> order low pass filter where  $K_{pv}$  is  $C_s \omega_{c1}$ . As shown in Fig. 10, if the feed-forwarding term is compensated with consideration of the 1<sup>st</sup> order low pass filter, the transfer function of the 2<sup>nd</sup> stage can be expressed as the 2<sup>nd</sup> order low pass filter.

$$\frac{\omega_{c1}}{s + \omega_{c1}} \begin{bmatrix} sK_{pd} + K_{id} & K_{idq} \\ K_{iqd} & sK_{pq} + K_{iq} \end{bmatrix} \begin{bmatrix} i_{ds}^r - i_{ds}^r \\ i_{qs}^r - i_{qs}^r \end{bmatrix} = \begin{bmatrix} s(sL_{ds} + R_s) & -\omega_r L_q \\ \omega_r L_d & s(sL_{qs} + R_s) \end{bmatrix} \begin{bmatrix} i_{ds}^r \\ i_{qs}^r \end{bmatrix} \quad (8)$$

$$\begin{bmatrix} i_{ds}^r \\ i_{qs}^r \end{bmatrix} = \begin{bmatrix} \frac{\omega_{c1}\omega_{c2}}{s^2 + \omega_{c1}s + \omega_{c1}\omega_{c2}} & 0 \\ 0 & \frac{\omega_{c1}\omega_{c2}}{s^2 + \omega_{c1}s + \omega_{c1}\omega_{c2}} \end{bmatrix} \begin{bmatrix} i_{ds}^r \\ i_{qs}^r \end{bmatrix} \quad (9)$$

$$\begin{bmatrix} v_{ds\_ff}^r \\ v_{qs\_ff}^r \end{bmatrix} = \frac{s + \omega_{c1}}{\omega_{c1}} \begin{bmatrix} 0 \\ \omega_r \lambda_{PM} \end{bmatrix} = \begin{bmatrix} 0 \\ \omega_r \lambda_{PM} \end{bmatrix} \quad (10)$$

From equation (8), if P gain ( $K_{pd}, K_{pq}$ ) is set as  $L_{ds} \omega_{c2}, L_{qs} \omega_{c2}$  respectively, and I gain ( $K_{id}, K_{iq}$ ) is set as  $R_s \omega_{c1}$  and coupled integrator gain ( $K_{idq}, K_{iqd}$ ) is set as  $-\omega_r L_{qs} \omega_{c2}, \omega_r L_{ds} \omega_{c2}$  respectively, the transfer function can be derived as (9) where the feed forwarding ( $v_{dqs\_ff}^r$ ) term is (10).

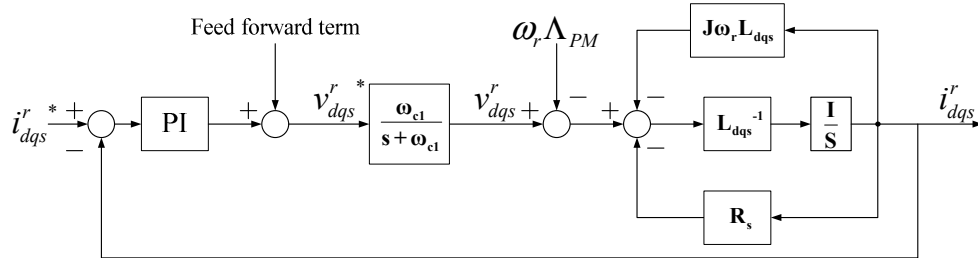


Fig. 10: Block diagram for two stage modeling

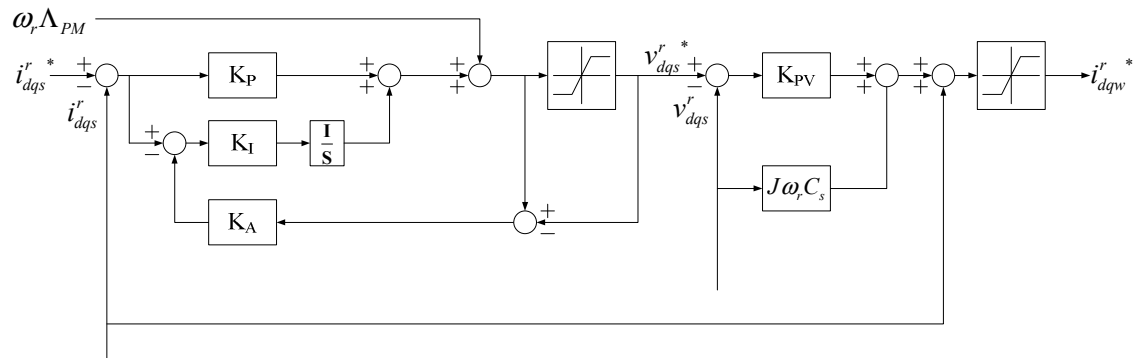


Fig. 11: Block diagram of designed multi-loop controller

In addition to the proposed multi-loop current control scheme in Fig. 11, virtual resistor ( $R_d$ ) can be implemented in the designed current controller. As shown in Fig 12, the virtual resistor can be easily added to the feed-forwarding term together with simple modification of the integrator gain.

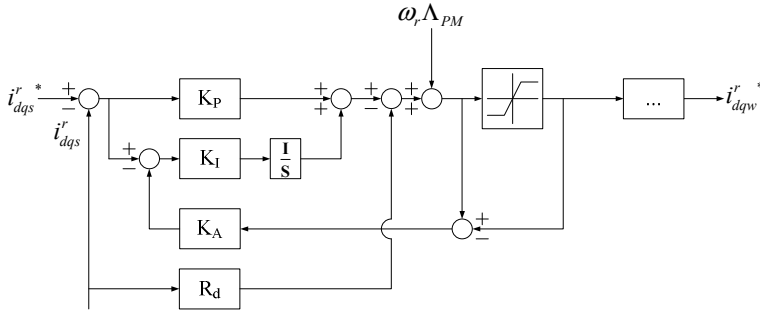


Fig. 12: Multi-loop current controller with series connected virtual resistor

### Power Control Strategy

There might be many possible choices as power control strategy. In this paper, for the control strategy of power, the DC link current is controlled by each CSC of grid side and the wind power is controlled by each CSC of wind turbine generator side. And it is assumed that the generated power by wind turbine can be known as soon as possible with high speed communication or measuring DC link voltage and current in order to minimize the current fluctuation in DC-link. Fig. 13 depicts the proposed DC-link current controller. The DC-link current is controlled by the grid side active current,  $i_{qs}^r$ , and the feed-forwarding term can provide additional active current, which is derived by the generated power of PMSG, to the grid in order to minimize DC-link current fluctuation.

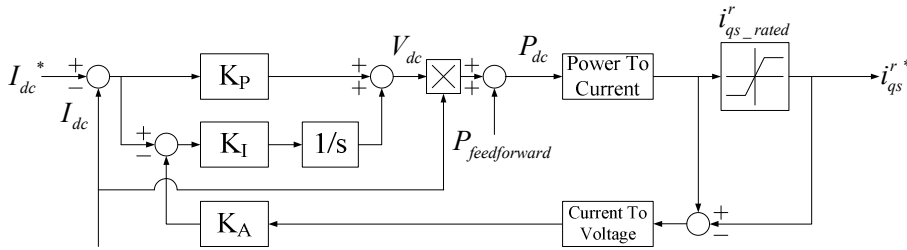


Fig. 13: DC-link current controller

### PWM strategy

To generate gating signals, the space vector pulse width modulation (SVPWM) for CSC is adopted [12]. To achieve the proposed current control, measurement of the average voltage is important in a switching period with the switching frequency over 1 kHz. There are several options for the placement of zero current vector in a switching period. To measure the average value of phase voltage in filter capacitor, the center aligned zero current vector placement was used in this study.

Fig. 14 shows the sampling point and zero current vector placement.  $I_0$  stands for the zero current vector, and  $I_n, I_{n+1}$  stand for the effective current vector.

To minimize ripple current in grid side and DC-link inductor, the interleaving method can be adopted using phase shifted carrier. Due to the characteristics of series connection, the switching ripple current can be extremely diminished as the number of series connected CSCs increases.

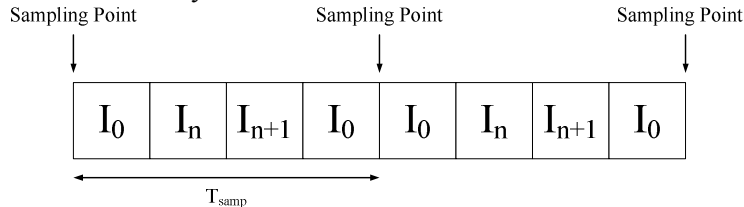


Fig. 14: Center aligned zero current vector

### Simulation Results

To verify the feasibility of the proposed configuration and control strategy, the computer simulation has been performed using PSIM software. The parameters for simulation have been shown in Table I. Under the assumption of 1700 V IGBT and diode as the switching device, 2 kHz is used as switching



frequency. Three CSCs connected to 9-phase PMSG is tied to the grid via DC current link, and the generator operates at the rated speed, 20 Hz, and the rated current. And three CSCs with the ideal multi-winding transformer is used for the grid side connection. The PWM carrier of series connected CSC has been interleaved by 120 degree phase shift to each other. With the series connection of 1 MW CSC, total 3 MW can be transmitted from 9 phase PMSG to the grid. And the total DC-link inductance in series is 3 mH.

**Table I: System parameters**

Rated Power of CSCs	1 MW
Rated line-to-line voltage	690 V <sub>rms</sub>
Rated phase current	836 A <sub>rms</sub>
<b>Generator Parameters</b>	
Stator resistance	0.01 Ohm (0.02 pu)
Synchronous inductance	1.1 mH (0.3 pu)
Rated frequency	20 Hz
<b>Converter Parameters</b>	
Y-connected Generator side capacitance	835 μF (0.05 pu)
Y-connected Grid side capacitance	835 μF (0.15 pu)
Grid side filter inductance	0.25 mH (0.2 pu)
DC-link inductor	3 mH

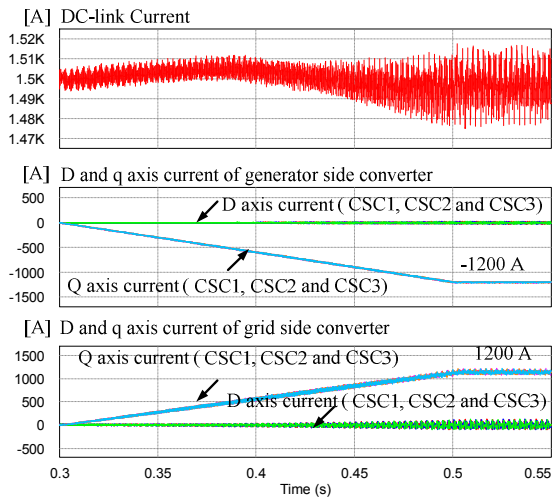


Fig. 15: DC-link current and d,q axis current of generator and grid side

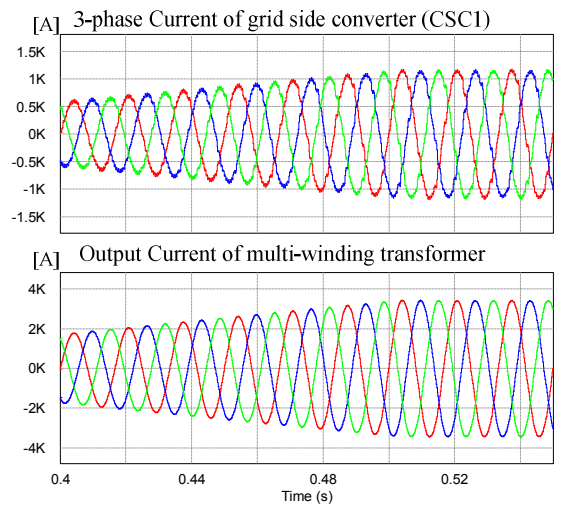


Fig. 16: Interleaving effect with 9-phase multi winding transformer

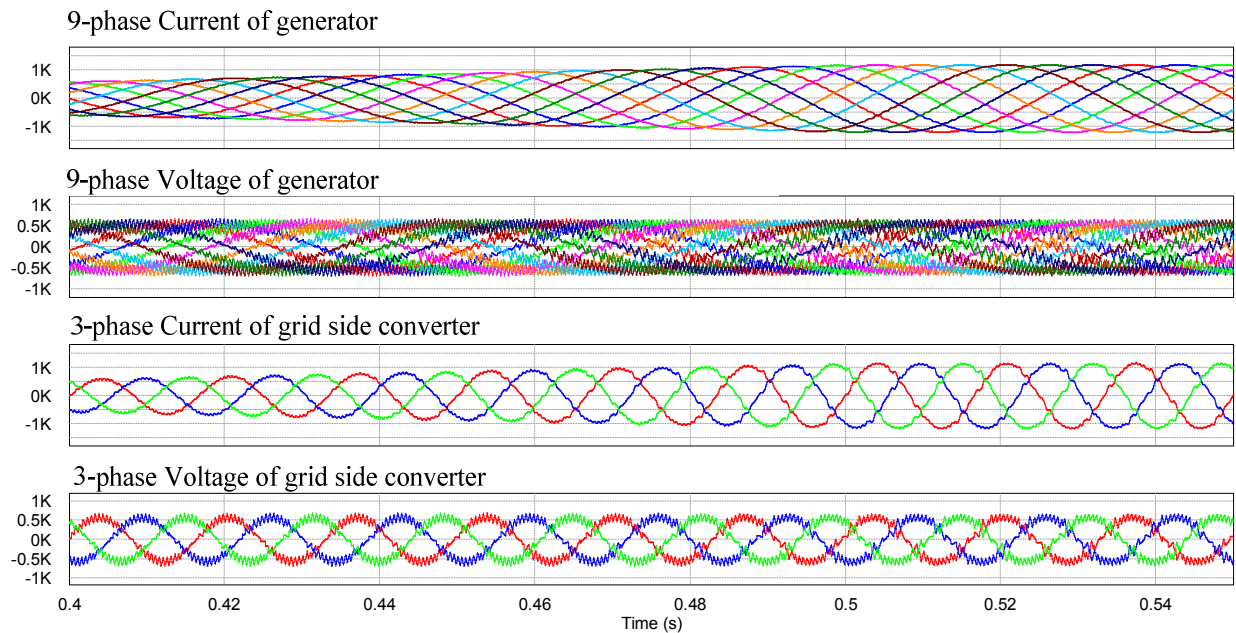


Fig. 17: Phase current and voltage of generator and grid side

The DC-link current regulation performance is revealed in Fig. 15. Each CSC of the generator side provides the rated power (rated  $q$  axis current) to DC-link, and each CSC of grid side regulates DC-link current.

In Fig. 16, the total sum of phase current of grid side converter, which is the output current of the multi-winding transformer, is shown. The output 3-phase current is almost pure sinusoidal one due to the interleaving effect with the carrier shifted PWM.

Fig. 17 shows all 9-phase currents, 9-phase voltage of PMSG and 3-phase current and 3-phase voltage of the multi winding transformer of the grid.

## Conclusion

In this paper, the Series Connected Current Source Converter system for variable speed full scale WTGS has been proposed. The SCCSC system can be easily incorporated with the multi-phase PMSG and the multi winding transformer. SCCSC system can be enlarged to integrate multiple WTGSs in the wind farm via medium voltage DC current link. Though each winding of PMSG should be insulated to the medium voltage, the power from multiple WTGSs can be transmitted without additional step-up transformer, AC/DC, and DC/AC converters for DC transmission, which are need to implement DC voltage transmission with the parallel connected VSC based WTGS. Due to the modularity of SCCSC as well as series concept, the 1700 V class IGBT and diode can be used as the power semiconductors of SCCSC, and the cost effectiveness and higher reliability can be achieved simultaneously. To dampen the LC resonance, the multi-loop current controller has been used. To evaluate the performance of the proposed configuration and control strategy, computer simulation has been performed using PSIM software. The simulation results proved the possibility of reasonable DC and AC current regulation with three series connected CSCs with PMSG whose total power is 3 MW.

## References

- [1] A. Pullen (2010. Sep.). Global wind capacity to reach close to 200 GW this year (Latest news). [Online]. Available : <http://www.gwec.net>
- [2] S. Muller, M. Deicke and R. W. De Doncker, "Doubly fed induction generator systems for wind turbines," *IEEE Ind. Applications Magazine*, vol. 8, no. 3, pp. 26-33, Jun. 2002.
- [3] Z. Chen, J. M. Guerrero and F. Blaabjerg, "A review of the state of the art of power electronics for wind turbines," *IEEE Trans. Power Electronics*, vol. 24, no. 8, pp. 1859-1875, Aug. 2009.
- [4] G. F. Conroy and R. Watson, "Low-voltage ride-through of a full converter wind turbine with permanent magnet generator," *IET Renew. Power Gener.*, vol. 1, no. 3, pp. 182-189, Sep. 2007.
- [5] H. Polinder, F. F. A. van der Pijl, G. J. de Vilder, and P. J. Tavner, "Comparison of direct-drive and geared generator concepts for wind turbines," *IEEE Trans. Energy Convers.*, vol. 21, no. 3, pp. 725-733. Aug. 2006.
- [6] H. Li and Z. Chen, "Overview of different wind generator systems and their comparisons," *IET Renew. Power Gener.*, vol. 2, no. 2, pp. 123-138. Jun. 2008.
- [7] S. A. Richter, B. Bader, and R.W. De Doncker, "Control of high power PWM current source rectifier," in *Proc. IPEC-2010*, pp. 1287-1292, Jun. 2010.
- [8] M. Salo, H. Tuusa, "Vector-controlled PWM current-source-inverter-fed induction motor drive with a new stator current control method," *IEEE Trans. Industrial Electronics*, vol. 52, no. 2, pp. 523-531, Apr. 2005.
- [9] H. Bilgin and M. Ermis, "Design and implementation of a current-source converter for use in industry applications of D-STATCOM," *IEEE Trans. Power Electronics*, vol. 25, no. 8, pp. 1943-1957, Aug. 2010.
- [10] B. Andresen and J. Birk, "A high power density converter system for the Gamesa G10x 4.5 MW wind turbine," in *Proc. 2007 European Conf. Power Elec. And Appl.*, pp. 1-8, Sept. 2007.
- [11] F. Briz, M. W. Degner and R.D. Lorenz, "Analysis and design of current regulators using complex vectors," *IEEE Trans. Industrial Applications*, vol. 36, no. 3, pp. 817-825, May/June 2000.
- [12] Y. W. Li, B. Wu, D. Xu and N. R. Zargari, "Space vector sequence investigation and synchronization methods for active front-end rectifiers in high-power current-source drives," *IEEE Trans. Industrial Electronics*, vol. 55, no. 3, pp. 1022-1034, Mar. 2008.